Italian Journal of Geosciences (2019) 138 (2): 184–201. https://doi.org/10.3301/IJG.2018.35

LOW-ANGLE NORMAL FAULTS RECORD EARLY PERMIAN EXTENSIONAL TECTONICS IN THE OROBIC BASIN (SOUTHERN ALPS, N ITALY)

A. Zanchi[1], S. Zanchetta[1*], L. Berio[1,2], F. Berra[3] & F. Felletti[3]

[1]*Dipartimento di Scienze dell'Ambiente e della Terra, Piazza della Scienza 4, 20126 Milano, Italy*

[2]*Dipartimento di Scienze Chimiche, della Vita e della Sostenibilità Ambientale, Parco Area delle Scienze 157/A, 43124 Parma, Italy*

[3] *Dipartimento di Scienze della Terra "A. Desio", Via Mangiagalli 34, 20133 Milano, Italy*

*corresponding author: Stefano Zanchetta
Address: Dipartimento di Scienze dell'Ambiente e della Terra, Piazza della Scienza 4, 20126 Milano, Italy.
Mail: stefano.zanchetta@unimib.it
Tel.: +39 02 6448 2063
Fax: +39 02 6448 2073
Skype: stefano.zanchetta

ABSTRACT

Well-preserved SSE-dipping low-angle normal faults (LANF) active during the Early Permian (Cisuralian) were recognized along the northern margin of the Orobic Basin (central Southern Alps, N Italy). These faults, which escaped most of the Alpine deformations, exhumed the Variscan basement during the deposition of the upper part of the Lower Permian succession (Pizzo del Diavolo Formation). Fault planes show evidence of frictional processes typical of the upper crust associated with hydrothermal circulation, responsible for the deposition of cm to m thick tourmalinite and Uranium mineralization.

The recognized LANFs interacted with high-angle normal faults producing half grabens that stored the Lower Permian deposits, where synsedimentary fault activity in their hangingwall is testified by abrupt vertical and lateral facies changes, thickness variations and by soft-sediment deformations. Mesoscopic structures, exposed in the hangingwall of a major LANF (the Aga-Vedello Fault system) along a synthetic high-angle normal fault, include conjugate normal faults, horst-and-graben, domino-

style planar and listric faults, which clearly record synsedimentary deformations testified by liquefaction and dewatering structures, typical of pre-consolidation hydroplastic conditions. This exceptional record indicates deformations at shallow crustal level which occurred during the Early Permian along high-angle normal faults soling into the LANFs, forming the northern boundary of the Orobic Basin.

The outcrop continuity, the perfectly preserved relationships among high- and low-angle normal faults together with the synsedimentary record of fault activity and the occurrence of mesoscopic faults developed during the deposition of the sediments, make this case-study an excellent reference for the analysis of extensional tectonics in synsedimentary conditions.

In addition, the occurrence of large LANF systems, typical of a stress regime characterized by a vertical σ_1, suggests that the Lower Permian Orobic Basin was dominated by pure extension at least in the study area, alternatively to existing interpretations, which favor a transtensional origin of the basin. Strike-slip tectonics can be responsible for a later partial tectonic inversion of the basin, as testified by the angular unconformity with the overlying Upper Permian succession (Verrucano Lombardo), marking a Middle Permian stratigraphic gap.

INTRODUCTION

The post-Variscan evolution of the Southern Alps records several episodes of crustal extension starting in the Early Permian and culminating in the Early Jurassic rifting, affecting the Adria passive margin (BRODIE *et alii* 1989; DIELLA *et alii*, 1992; HANDY *et alii*, 1999; BERRA & CARMINATI, 2009), that finally led to the opening of the Alpine Tethys (BERNOULLI & WINKLER, 1990; BERTOTTI *et alii*, 1993; BERRA *et alii*, 2009). The occurrence of extensional processes between the end of the Triassic and the Early Jurassic is described in several contributions dealing with evidence of synsedimentary tectonics (BERNOULLI, 1964; BERTOTTI *et alii*, 1993; BERRA & CARMINATI, 2009) along the western margin of the central Southern Alps. Late Triassic - Jurassic extensional faults are characterized by high-angle and low-angle surfaces within the sedimentary cover, or between the sedimentary cover and the basement, passing to intra-basement shear zones (BERTOTTI *et alii*, 1993; REAL *et alii*, 2018). The existence of highly subsiding, fault-controlled basins in form of isolated grabens bounded by steep normal faults in the Cisuralian (Lower Permian) succession of the central Southern Alps (CASATI & GNACCOLINI, 1967; CADEL, 1986; CADEL *et alii*, 1996; CASSINIS *et alii*, 1986; 2012; BERRA *et alii*, 2015, 2016) documents an older major extensional event, generally ascribed to transtensional tectonics by most of the authors. The connected geodynamic framework has been related to a dextral megashear zone active between Laurussia and Gondwana (ARTHAUD & MATTE, 1977; DOMEIER & TORSVIK, 2014), that dismembered the Variscan belt during the Permian (ZIEGLER, 1993; HANDY & ZINGG, 1991; EDEL *et alii*, 2018), taking to the transformation from Pangea-A to Pangea-B (MUTTONI *et alii*, 2003, 2009).

The occurrence of Early Permian low-angle normal faults has been recently documented in the western cSA (e.g.: Grassi detachment, FROITZHEIM *et alii*, 2008) suggesting a major role of extensional phenomena during the deposition of the Lower Permian successions.

Evidence of Early Permian syndepositional tectonic activity was recognized in the central Southern Alps by normal faults associated to abrupt facies and thickness changes in the volcanic-siliciclastic successions of the Lower Permian succession (CADEL *et alii*, 1996; CASSINIS *et alii*, 2012; ISPRA 2012a, 2012b; BERRA *et alii*, 2016) and by earthquakes-triggered soft-sediment deformations (BERRA & FELLETTI, 2011).

During the later Alpine compression, favourably oriented normal faults inherited from Permian tectonics played an important role, being frequently inverted as south-verging thrusts (BLOM & PASSCHIER, 1997; ZANCHETTA *et alii*, 2015). Despite the polyphase Alpine tectonics (MILANO *et alii*, 1988; ALBINI *et alii*, 1994; SPALLA *& Gosso*, 1999), several Permian structures exposed at the head of the Brembana Valley (BG) escaped the Alpine deformation, thus preserving their original features. Based on original structural analyses and mapping in the highest part of the Brembana Valley, in this paper we document two of the clearest examples of these structures, which consist of low-angle well-preserved Early Permian normal faults (LANF). These two faults were associated to high-angle synsedimentary normal faults active during the deposition of the upper part of the Lower Permian succession. In order to characterize these fault systems from a structural point of view, we performed detailed geological mapping (1:2,000 scale) accompanied by mesoscopic analyses of synsedimentary faults and associated liquefaction structures formed in hydroplastic conditions. Our fieldwork was completed by the microstructural analyses of the fault rocks formed along the two LANFs and of the related tourmalinites, which characterize these fault systems. Obtained results were integrated in the stratigraphic framework recently suggested by BERRA *et alii* (2016) for the upper portion of the Lower Permian deposits.

The reconnaissance of a preserved Early Permian synsedimentary fault system characterized by the occurrence of LANFs (dip < 30°), which formed the northern tectonic boundary of the Orobic Basin entails important implications also on the Early Permian evolution of the basin, as they are mostly related to a tectonic regime dominated by pure extension rather than by transtension as previously mentioned. Another point of interest of this work is given by the analysis of synsedimentary faults developed in hydroplastic conditions, which represent a significant case study of soft-sediment deformations possibly developed in a seismic context.

GEOLOGICAL SETTING

The central Southern Alps are a fold-and-thrust belt (SCHÖNBORN, 1992; CARMINATI *et alii*, 1997; ZANCHETTA *et alii*, 2015) deeply involving a polyphase Variscan basement (MILANO *et alii*, 1988; SPALLA *& GOSSO*, 1999) and its upper Palaeozoic to Cenozoic sedimentary cover. A polyphase Alpine deformational history, occurring between the Cretaceous and the uppermost Miocene marks the southward stacking of the thrust sheets (BRACK, 1981; SCHÖNBORN, 1992; FANTONI *et alii*, 2004; ZANCHETTA *et alii*, 2011, 2015; D'ADDA & ZANCHETTA, 2014), which mainly occurred in brittle conditions with no significant metamorphism (e.g.: CARMINATI & SILETTO, 2005).

In the northern area of the belt, the Variscan basement is stacked along the Orobic-Gallinera Thrust System (Fig.1) on the Permian-Mesozoic succession of the northern portion of the Orobic Anticlines *s.l.* This system forms a set of ENE-WSW dextral *en échelon* anticlines exposing the basement and the Carboniferous to Lower Triassic successions between the Orobic-Gallinera Thrust System to the north and the Valtorta-Valcanale Fault to the south (Fig.1); the latter separates these units from the imbricated Mesozoic carbonates to the south.

The Orobic-Gallinera Thrust System, in the study area, branches out interacting with a bundle of ENE-WSW trending faults, interpreted as reactivated Lower Permian extensional faults (ZHANG *et alii*, 1994; CADEL *et alii*, 1996; BLOM & PASSCHIER, 1997).

The Permian sedimentary succession consists of two major sedimentary systems separated by an angular unconformity: (i) an older system represented by the Lower Permian volcanic and terrigenous units of the Laghi Gemelli Group, which is unconformably covered by (ii) a younger system, consisting of the Upper Permian continental red beds of the Verrucano Lombardo (Fig. 2). The older system (recently revised by BERRA *et alii*, 2016) includes several units, starting at the base with the up to 100 m, pre-volcanic, thick Basal Conglomerate, covered by the up to 800 m thick Cabianca Volcanite (CBV), including large ignimbrite sheets (284 to 270 Ma; BERRA *et alii*, 2015). The CBV is covered by the Pizzo del Diavolo Formation (PDV), which consists, in the central part of the Orobic Basin, of coarse-grained proximal conglomerates (Mt. Aga Conglomerate, AC, to the north and Val Sanguigno Conglomerate to the south) passing to fine-grained deposits (volcaniclastic sandstone and dark mudstone) in the depocentral area of the basin. Tetrapods footprints in the PDV suggest a latemost Kungurian age (PETTI *et alii*, 2014; MARCHETTI *et alii*, 2017). Stratigraphic and tectonic evidence points to an intracontinental fault-controlled basin developed in semi-arid conditions, strongly recalling the present-day Basin and Range Province (BERRA *et alii*, 2016). The younger system consists of Upper Permian (Lopingian) red sandstones and conglomerates of Verrucano

Lombardo, unconformably covering the Lower Permian succession along a marked angular unconformity, testifying to deformation and deep erosion of the Laghi Gemelli Group (CASATI & GNACCOLINI, 1967; BERRA *et alii*, 2016).

BASIN ARCHITECTURE AND EVIDENCE OF SYNDEPOSITIONAL TECTONICS IN THE OROBIC BASIN

The stratigraphy and architecture of the Permian Orobic basin was analyzed in details by several authors, starting from the pioneering work by DE SITTER & DE SITTER-KOOMANS, (1949). Rapid changes in thickness and facies distribution reflect Permian syndepositional tectonic activity, responsible for the development of E-W oriented faults and related facies belts (CASATI & GNACCOLINI, 1967; CADEL *et alii*, 1996) in a semi-arid depositional setting (BERRA *et alii*, 2016). The northern margin of the Orobic Basin is marked by the Mt. Aga Conglomerate, which is in tectonic contact with the Variscan basement along the Aga-Vedello LANF, bordering the basin to the north. The Mt. Aga Conglomerate consists of poorly selected angular to subangular basement clasts (ZANONI *et alii*, 2010; ZANONI & SPALLA, 2018) with subordinate volcanic fragments of the CBV, reflecting deposition of coarse proximal alluvial fans.

Thickness and facies changes of the CBV and PDV indicate that different syndepositional faults were active during deposition. A strong evidence of fault-controlled subsidence (Fig. 2) is documented by the sharp decrease of the thickness of the CBV (CADEL *et alii*, 1996) from about 800 m to 100-200 m across the steep Fregabolgia Fault (Fig. 2).

The abrupt thickness and facies changes in the CBV across the Fregabolgia Fault suggest that this fault was an Early Permian high-angle normal fault reactivated during the Alpine evolution. After the end of the emplacement of the ignimbritic flows of the CBV, the area south of the Fregabolgia Fault became a relative topographic high, likely during the deposition of the PDV. CADEL *et alii* (1996) consider the Fregabolgia Fault as the border of a large Permian caldera, which formed during the deposition of the Cabianca ignimbrites.

Thickness changes are also observed in the PDV. Unequivocal evidence of syndepositional tectonics during the deposition of the PDV occurs at mesoscopic scale, consisting of common soft-sediment deformations (seismites) observed in different part of the basin, more abundant at specific stratigraphic positions (BERRA & FELLETTI, 2011). The overall evolution of the PDV records a general fining-upward trend, with the upper part represented by volcaniclastic sandstones and siltstones containing carbonate layers. This evolution suggests an enlargement of the basin in time and possibly a progressive decrease of the tectonic activity. The upper boundary of the PDV is represented by an angular unconformity (reflecting post-depositional deformation), sealed by the Upper Permian fluvial deposits of the Verrucano Lombardo.

THE LOWER PERMIAN LOW-ANGLE NORMAL FAULTS

Two major low-angle normal faults (Aga-Vedello and Masoni LANFs, Fig. 2) document the early Permian extension, recorded by the PDV sediments along the northern border of the Orobic Basin. They are *non-Andersonian* low-angle normal faults (LANFs), which juxtapose the PDV succession (Mt. Aga Conglomerate, slates and sandstones in the hangingwall) directly on the Variscan basement in the footwall. The angle between the bedding in the sediments and the fault plane ranges from 5° to 15° (Figs. 3 and 4). Extensional horses including thin slices derived from the Cabianca Volcanite often occur between the basement and the AC, especially along the Masoni LANF. Pervasive hydrothermal fluid circulation, that accompanied the activity of the Lower Permian extensional faults, is testified by the occurrence of tourmalinites and U-bearing minerals impregnating cataclasites formed along the basement-cover fault contact (ZHANG *et alii*, 1994; DE CAPITANI *et alii*, 1999). Both the Masoni and the Aga-Vedello LANFs are overthrust by Alpine thrust sheets, which stack the Permian succession southward (Fig.1 and 2).

The Aga-Vedello LANF represents the most important structure of the area and continues eastward across the Vedello Valley (Fig. 1) forming the northern margin of the Lower Permian Orobic Basin (CADEL *et alii*, 1996). The fault is continuously exposed for kilometers around the western slopes of Mt. Aga above the Lago del Diavolo (Figs. 5a, 5b) along the northern base of the steep rock walls, which form the impervious ridges between the Cigola Pass and the Vedello Valley.

The Masoni LANF (Fig. 2 and Fig. 6) can be followed around Mt. Masoni from its norther slopes to the south, where it is crosscut by high-angle reverse faults. This fault, which was described in detail by BLOM & PASSCHIER (1997), is severely folded eastward, whereas it is perfectly preserved in its western portion; here, it was only gently bent during the Alpine compression forming an open E-W trending syncline half-kilometer wide. The Early Permian fault is overthrust by a thrust sheet consisting of Verrucano Lombardo and Servino, forming the top of Mt. Masoni and rooting northward within the basement (Fig. 6a and 6b).

A second type of Lower Permian faults consists of ENE-WSW-trending NNW-dipping high-angle normal faults , partially inverted as reverse faults (as indicated by kinematic indicators, cleavage and folds in the hangingwall) during the Alpine shortening but still showing younger-on-older relationships (e.g. Cigola-Longo and Fregabolgia faults; Fig. 2, 3).

The interaction of the high- and low-angle normal faults results in an asymmetric architecture of the basin, which consists of a composite major half-graben (roughly 10 to 20 km wide), divided by minor horsts in smaller sub-basins. The two main asymmetric sub-basins extend between the Mt. Masoni LANF and the Cigola-Longo Fault and between the Aga-Vedello LANF and the Val Camisana and Fregabolgia faults (Fig.2).

The Lower Permian synsedimentary fault activity is documented by sedimentological and tectonic evidence along the western slopes of Mt. Aga, close to the Cigola Pass (Fig. 3, 4). The Aga-Vedello LANF, which is here perfectly exposed, shows a clear interaction with a SSW-dipping high-angle normal fault in its hangingwall (Fig. 4). This fault, which merges into the underlying LANF, is a growth fault (Aga Growth Fault; Figs. 5, 7) with the footwall consisting of the Mt. Aga Conglomerate and the volcaniclastic sandstones of the PDV, whereas its hangingwall displays a thicker succession, with downward-displaced conglomerates and sandstones with interposed slates, which rapidly pinch out westward (Fig.3, 4). In addition to major thickness variations of the deposits across the fault, perfectly preserved brittle and hydroplastic mesoscopic structures are exposed along the fault zone, suggesting that tectonic activity was recorded by different types of structures.

Mesoscopic evidence of normal faults was observed both in the hangingwall of the Masoni LANF (just below the top of Mt. Masoni) and in the hangingwall of the Cigola-Longo Fault, where conjugate systems, although severely shortened and tilted due to Alpine folding, can still be recognized. Mesoscopic secondary fault planes along these major faults follow the strike of the master faults.

FAULT-RELATED STRUCTURES AND TOURMALINITES OF THE AGA-VEDELLO AND MASONI LANFS

LANFs planes are well exposed in the Lago del Diavolo and Mt. Masoni areas (Fig. 2), where several outcrops record fault-related structures at the mesoscale. Fault surfaces are planar at the meter scale: they are characterized by cataclastic deformations that mainly affect the metamorphic basement in the footwall. The typical structure (Fig. 8a and 8b) of fault planes consists of a cataclastic band, 1 to 15 cm thick, developed at the expense of the Variscan basement gneiss, which is usually overlain by a thin layer (7-8 cm, up to 20 along the Masoni LANF, Fig. 8b) of dark grey to black aphanitic tourmalinite. A cataclastic layer consisting of volcaniclastic sandstone and/or conglomerate of the PDV develops in the hangingwall of the fault plane. Tourmalinites are usually located along the contact between basement-derived and cover-derived cataclasites (Fig. 8a, 8b and 8c).

Gneiss-derived cataclasites are both matrix- and clast-supported (Fig. 8c and 8d), with the former being by far the more frequent. Clasts within cataclasites mainly consist of polycrystalline quartz aggregates and K-feldspar, with very rare tourmaline clasts up to 2-3 mm in size. These clasts of tourmaline (Fig. 8d) likely derived from tourmaline crystals of metamorphic origin that are common within the leucocratic Corno Stella Gneiss.

Both foliated and non-foliated cataclasites occur (Fig. 8d, 8e and 8f), with the latter overprinting foliated precursors. This likely testifies to a protracted fault activity, with fabrics formed at shallow crustal level that overprint the ones formed at depth.

Tourmalinites (TRM) almost invariably occur along fault zones and likely formed in response of metasomatic processes due to B- and Al- rich fluids that migrated along fault planes (ZHANG *et alii*, 1994; SLACK *et alii*, 1996; DE CAPITANI *et alii*, 1999). Such fluids impregnated cataclasites, usually overprinting existing fault textures that are almost completely obliterated except for rare relict clasts. Porphyroclasts in the studied samples are made of coarse-grained polycrystalline quartz and/or K-feldspar, pointing to the Corno Stella Gneiss as their source. The obliteration of cataclastic fabric and the lack of deformation, except for the occurrence of an Alpine cleavage discussed below, suggest that TRM formation postdated the main fault activity, as already observed by ZHANG *et alii* (1994).

Foliation in cataclasites derived from the PDV is usually more pervasive with respect to basement-derived cataclasites, even if differences between cataclastic foliation and Alpine cleavage is not always clear. A superposed cleavage is evident (Fig. 6c) where the fault was clearly folded and deformed during Alpine deformations along the northern branch of the Masoni LANF (see also BLOM & PASSCHIER, 1997). Also, along several segments of the Aga LANF, an Alpine cleavage, often associated with small-scale crenulation folds, is clearly superposed on the cataclastic layers. The cleavage becomes less pervasive in TRM veins and in basement-derived cataclasites, where it usually disappears within 50 to 100 cm from the fault planes due to rheological contrast between the very low-grade terrigenous sediment of the cover and the gneissic basement. A cleavage refraction commonly occurs across cataclasites-TRM bands, being steeper within TRM and basement-derived cataclasites and at a lower angle in cataclastic rocks from the PDV. The Early Permian age of the TRM is documented by the presence of clasts of TRM in the basal part of the Verrucano Lombardo, documenting the erosion and resedimentation of these fault-related rocks before the Late Permian (BORIANI *et alii*, 2016; BARGOSSI *et alii*, 2016).

Microstructures and compositional features of cataclasites and tourmalinites

Cataclasites chiefly derive from the Corno Stella Gneiss. Studied samples invariably show a matrix-supported texture, with matrix abundance of 50-90 %. Clasts are rounded to sub-rounded with a prevalent size of 100-150 μm with subordinate larger grains (Fig. 8d, 8e and 8f).

Fault-related structures of Permian age are well preserved along both the Aga-Vedello and Masoni LANF. The only exception is the northern part of Masoni LANF, where the original structure is overturned due to Alpine folding. Here the Permian cataclasites are re-activated as a reverse shear zone, along which minor recrystallization of fine-grained quartz and white mica (Fig. 8e and 8f) forms a protomylonitic foliation.

The cryptocrystalline nature of TRM, already described by ZHANG *et alii* (1994), SLACK *et alii* (1996) and DE CAPITANI *et alii* (1999), was confirmed by our observations at the optical and electron scanning microscopes. For the study of microstructural and compositional features of TRM veins we selected samples not affected by Alpine deformation. Based on optical observations, TRM veins are made of 50-70 % in volume of an aphanitic matrix consisting of extremely fine-grained (< 0.02 μm) tourmaline crystals, in which subrounded clasts, mainly made of quartz, occur (Fig. 8g and 8h). The remaining volume consists of relicts of gneiss-derived cataclasites, usually displaying minor tourmalinitization (DE CAPITANI *et alii*, 1999), as shown by the crystallization of thin tourmaline rims around some clasts (Fig. 8g). Large (> 10 μm) euhedral tourmaline crystals seldom occur within the cryptocrystalline matrix. These crystals are homogeneous in composition and usually lack the thin overgrowth rims observed on tourmaline clasts within cataclasites.

Microstructural observations, together with X-ray element map analysis (Fig. 8h), show that tourmalinites formed from B- and Al-rich fluids that migrated along cataclastic fault zones, precipitating cryptocrystalline tourmaline. The X-ray maps (Fig. 8h) clearly show an increase in Al, Fe, Mg and Na in TRM veins with respect to cataclasites, coupled with a significant decrease of Si that is removed from the system. The boundary between TRM bands and hosting cataclasites is usually sharp, with only thin irregular veins that branch out from the main one into surrounding cataclasites (Fig. 8h).

Electron microprobe analyses (see Table 1 for methods and results) were performed both on the matrix of TRM veins and on larger tourmaline crystals within them, as well as on tourmaline clasts within cataclasites (Fig. 8i). Matrix analyses have been reported only as oxides because the variable Si content suggests that, due to non-distinguishable grain size, these should be considered mixed analyses, in which the tourmaline composition is contaminated by the occurrence of other mineral phases, most likely quartz. Single crystals analyses (Table 1) have been instead re-calculated on the base of the following general formula $XY_3Z_6(BO_3)_3T_6O_{18}V_3W$ with X= Na, Ca, K, [ ]; Y= Mg, Fe^{2+}, Fe^{3+}, Li, Al, Mn, Ti^{4+}, Cr^{3+}; Z= Al, Mg, Fe^{3+}, Cr^{3+}; T=Si, Al; V=OH,O; W=OH, F, O (HAWTHORNE AND HENRY, 1999). B_2O_3 and H_2O have not been measured but have been recalculated based on stoichiometry considering 3 B atoms per formula unit. Tourmaline crystals within TRM veins display compositions belonging to the alkali-rich group of HAWTORNE & HENRY (1999), almost identical to the analyses reported by DE CAPITANI *et alii* (1999). In the Al-Fe-Mg classification diagrams, analyses plot, with a few exceptions, along the Schorlite-Dravite join with the cationic Mg/Fe ratio above 1 (Fig. 8i).

SYNDEPOSITIONAL TECTONIC DEFORMATIONS AT MT. AGA

Evidence of the Lower Permian syndepositional tectonics are abundant at the base of the PDV along the western slope of Mt. Aga (Fig. 3). We measured more than 250 mesoscopic fault surfaces (Fig. 7) whose displacement, evaluated by the throw of stratigraphic markers, ranges from a few millimeters to several meters (Fig. 9), both in the hangingwall and in the footwall of the Aga Growth Fault (Fig. 7). The distribution of the brittle, semi-brittle and plastic structures is strongly controlled by the physical properties of the sediments (e.g., grain size, degree of lithification and cohesivity) and by their resulting rheology. Frequency and distribution of these fault-related structures close to the fault surface indicate that their origin is clearly related to the multistage tectonic activity of the Aga-Vedello LANF and associated faults. Mesoscopic tectonic structures (symmetrical *Andersonian* conjugate faults forming horst-and-graben, regular dominoes, listric faults and coarse-grained breccias possibly due to hydro-fracturing) are recorded by cohesive or partly-lithified deposits, in close association with plastic deformations in fine layers. Liquefaction and dewatering structures (Fig. 10) as ball-and-pillow, flames, and sand dikes, give rise to an exceptional example of synsedimentary soft sediment tectonic deformation structures (SHANMUGAM, 2017 for a review) which decrease far away from the fault. Liquefaction, which occurs in shallow conditions (MONTENAT *et alii*, 2007) before sediment consolidation, possibly related to seismic shaking, testifies to fault activity during sedimentation.

The coexistence of plastic and brittle deformations in the same rock volume indicates that a complex pattern of deformation occurred during the activity along the fault system. A complete range of brittle to semi-brittle structures is exposed along fault planes, showing associations of regular and sharp surfaces (Figs.10a, d) passing to irregular fractures causing bedding disruption (Figs. 10b) and plastic dragging of coarse layers, whereas fine-grained beds are plastically deformed (Figs., 10b, c, e).

Typical hydroplastic structures as dish and pillows formed before the lithification of the sediment column (i.e.; at very shallow depth: < 20 m) and shortly after deposition, were successively displaced by brittle to semi-brittle faults (Fig. 10h). In other situations, faulting and liquefaction were strictly associated, as shown by flames occurring along or very close to the main fault surface or by plastic deformations (Fig. 10g).

These observations may suggest that the same fault slip event produced hydroplastic deformation close to the topographic surface along the fault and more brittle deformations at depth, the latter frequently associated with hydroplastic deformations generated by older events, when sediments were still plastic and closer to the depositional surface.

Mesoscopic fault populations (Fig.7), measured in an area of about 50 x 50 m, are dominated by high-angle conjugate sets of normal faults which have been gently tilted eastward due to Alpine folding. Geometrical relationships with bedding suggest that most of the faults were formed before block tilting when sediments were deposing on an almost horizontal surface. Faults mainly strike ENE-WSW, matching the strike of the Lower Permian master faults and displaying constant geometrical features, with the only exception of site s10 (Fig. 7), where dominant E-W to WNW-ESE trending fractures occur. The present-day attitude of fault populations is strictly related to bedding reorientation, which results from a combination of block tilting during the Permian fault activity and Alpine gentle folding. This is evident, e.g., at site s8 (Fig.7), where reverse faults result from a subsequent bending of the bedding surface (S_0). N-S to NE-SW trending fractures are interpreted as post-Permian fractures based on crosscutting relationships. Most of the faults still preserve a normal throw with a dominance of NNW-dipping surfaces, antithetic with respect to the Aga Growth Fault, accommodating deformation within the hangingwall. ENE-SSW trending conjugate systems which dominate mesoscopic fault associations generally show 2ϑ angles smaller than the typical *Andersonian* 60° value, all over the investigated area (Fig. 7). This can reflect an original mixed hybrid-shear failure mechanism due to fluid overpressure in unconsolidated sediments. Alternatively, it may result from the Alpine compression, which caused a marked steepening of fault planes, due to a strong shortening component roughly orthogonal to the fault surfaces.

The stratigraphic distribution of these structures suggests recurrent events of seismic shocks and fault activity during the deposition of the Mt. Aga Conglomerate the PDV, occurring when the sedimentary succession was buried by only a few meters of sediments. A similar setting with synsedimentary faults and liquefaction structures was described in the Pliocene volcaniclastic deposits exposed along an active fault related to the opening of the Gulf of California (ZANCHI, 1991), which were also interpreted to record syndepositional deformations along a fault scarp, possibly due to seismic shaking.

DISCUSSION

Seismic-scale exposures of preserved Permian syndepositional normal faults in the Orobic Basin allow defining in detail their original geometry and their role in controlling the basin evolution. After a major volcanic event (CBV), the Orobic Basin was characterized by the northward propagation of a SSE-dipping fault system (Aga-Vedello LANF), bordering the basin to the north (Fig. 11). During the deposition of the PDV, synsedimentary ENE-WSW trending faults, in present-day coordinates, defined strongly asymmetric half-grabens, resulting from the interaction of low- and high-angle normal faults (Fig. 12). These asymmetric basins were filled with a fining-upward continental succession, suggesting the enlargement of the basin with time and an increased subsidence southward. Syndepositional tectonics is recorded by abrupt thickness and facies changes and by associated spectacular soft-sediment deformations (Fig. 10), possibly ascribed to seismic shaking causing sediment liquefaction close to high-angle normal faults acting in the hangingwall of the Aga-Vedello LANF. Based on the above discussed lines of evidence, we propose that the analyzed LANF system can be interpreted as an upper crustal breakaway in the sense of WERNICKE (1981).

Hydrothermal activity affected the fault system during its development, which represented a preferential circulation path for B, Al and possibly also Hg and U (DE CAPITANI *et alii*, 1999). Hydrothermal fluids impregnated cataclastic layers suggesting a long-lasting fault activity during the exhumation of the fault to the surface from upper crustal depths (Fig. 12). Despite some uncertainties, recently performed U-Th-Pb radiometric ages on uraninite from the Novazza and Val Vedello mines provided a 275 ± 13 Ma age (MARTIN *et alii*, 2017), fitting with the presumed time of activation of the low-angle fault systems.

The most significant equivalents of the Lower Permian basins resulting from the interactions between low- and high-angle normal faults can be found, in terms of stratigraphic and structural settings, in the Basin and Range Province (e.g.: WERNICKE, 1981; DAVIS, 1986; LISTER & DAVIS, 1989). The Orobic Basin faults resemble the Black Mountains detachments, Death Valley (HAYMAN *et al.*, 2003), where high-angle synsedimentary normal faults sole into a low angle detachment (Fig. 12).

The classic interpretation of the Permian tectonics related to transtension caused by a dextral mega-shear zone active between Eurasia and Gondwana (e.g. ARTHAUD & MATTE, 1977; CASSINIS & PEROTTI, 1994; MUTTONI *et alii*, 2003) does not fit to the architecture of the Lower Permian succession of the Orobic Basin. It is well known from the literature (e.g.: COLLETTINI, 2011 for a review) that LANF are representative of a tectonic regime with a vertical σ_1, indicating pure extension (Fig. 12). Similarly, preserved or partially inverted crustal-scale LANF systems have been described in other areas of the central Southern Alps by FROITZHEIM *et alii* (2008), and ZANCHETTA *et alii* (2015).

A long-lasting discussion on the post-Variscan geodynamic setting has been going on since the end of the last century. Although the post-collisional Variscan evolution was often related to an extensional post-collisional collapse (e.g.: MENARD & MOLNAR, 1988; MALAVIEILLE *et alii*, 1990;

Malavieille, 1993; McCann *et alii*, 2006), most of the authors explains it with the activation of a large-scale dextral shearing between Laurussia and Gondwana (Arthaud and Matte, 1977; Ziegler, 1993; Handy & Zingg, 1991; Edel *et alii*, 2018 and ref. therein). This process, that dismembered the Variscan belt, resulted in a widespread transtensional tectonic regime well documented in the Central European area (e.g. Ziegler, 1993; McCann *et alii*, 2006).

Based on the large subsidence rates of the Lower Permian successions in the central Southern Alps and on the short life of the related basins, several authors (Cadel, 1986; Cadel *et alii*, 1996; Cassinis *et alii*, 2012; Berra & Carminati, 2009, Berra *et alii*, 2015, 2016) suggested that they were deposited within strike-slip dominated basins.

Conversely, we believe that the occurrence of LANFs typical of an extensional regime strictly recalling the Basin and Range Province of the USA strongly supports the importance of a strong lithospheric thinning, already invoked to justify the Permian-Triassic HT metamorphism affecting the Adriatic deep and intermediate crust (Marotta *et alii*, 2009). Extensional processes were also accompanied by a volcanic flare-up all along the Southern Alps during the beginning of the Permian (Schaltegger & Brack, 2007), as well as in most of the present-day Alpine region.

Our observations may suggest that crustal extension was particularly active during the initial stages of the development of the Permian basins. Alternatively, a strong partitioning between extensional and strike-slip fault systems occurred in the upper crust during the Early Permian, justifying the existence of domains characterized by pure extension in the Southern Alps, whereas strike-slip dominated basins were active to the north, in the European domain.

After the deposition of the PDV, the occurrence of a new deformational phase is testified by a marked angular unconformity (Casati & Gnaccolini, 1967; Berra *et alii*, 2016), which separates the Lower Permian units from the Upper Permian red beds of the Verrucano Lombardo. Strike-slip motions and transpressional deformations may have produced this unconformity probably related to a partial inversion and deformation of the Lower Permian basins, associated with the definitive conclusion of the magmatic activity.

The Permian tectonics also played an important role during the Alpine shortening, as discussed by previous authors (Cadel *et alii*, 1996; Blom & Passchier, 1997; Zanchetta *et alii*, 2015). The control on the development of Alpine thrusts is particularly evident in the study area, where the Orobic-Gallinera Thrust System branches out in several minor thrust surfaces following favourably oriented Permian faults (Fig. 2), which were inverted as high-angle dip-slip reverse faults. Inversion phenomena accommodated a limited amount of shortening along NNE-dipping high-angle normal faults, which can be distinguished as they always show younger-on-older stratigraphic relationships (e.g.: Fregabolgia and Cigola-Longo fault systems), as well as tight to isoclinal folding in the Lower

Permian succession of the hangingwall close to the fault surface. However, a large part of the shortening was accommodated by a newformed thrust surface passing north of the Orobic watershed from Mt. Masoni towards ENE, just to the north of the Aga-Vedello LANF (Fig. 1 and Fig 2).

S- to SE-dipping LANFs, due to their unfavourable attitude, were partially preserved just in the western part of the Mt.Masoni area and around Mt. Aga, where they are markedly oblique with respect to the main Alpine shortening direction. The occurrence of a stiff basement mainly consisting of the Corno Stella Gneiss in the footwall of the Aga-Vedello LANF may have contributed to the limited amount of finite strain of this area. High-angle normal faults surrounding Mt. Aga may have further contributed to disfavour the local reactivation of the LANF system as a back-thrust.

CONCLUSIONS

Detailed structural analyses performed along the uppermost Brembana Valley in the northern area of the Orobic Basin led to the recognition of an exceptionally preserved Permian fault system allowing for the analyses of the interactions among high- and low-angle normal faults active in a synsedimentary context during the deposition of the base of the PDV. The results of this study are summarized as follows:

- The northern boundary of the Lower Permian Orobic Basin is delimited by a low-angle fault system, which partially escaped Alpine deformation.

- The Aga-Vedello LANF, which extends westward to the Vedello Valley where it hosts an important U ore body, represents the major structure of this fault system.
- The well preserved fault surfaces are characterized by fine-grained cataclasites impregnated by tourmalinites, attesting a strong hydrothermal activity along fault zones.
- Interaction between low- and high-angle normal faults resulted in asymmetric half-grabens, deepening toward the basins depocenters (south).
- Rapid facies and thickness variations, liquefaction structures and mesoscopic synsedimentary faults formed in hydroplastic conditions at very shallow levels.
- The occurrence of LANFs, typical of a stress regime with a vertical σ_1, suggests a dominance of pure extension on transtension during the Early Permian in the Orobic Basin. In this context, LANFS activation might be related to a strong partitioning between extensional and strike-slip fault systems.

Acknowledgements

We warmly thank the two reviewers M. Barchi and I. Spalla for their constructive comments, which helped to improve the manuscript. This work was supported by FA grants to AZ and SZ, University of Milano-Bicocca. AZ dedicates this work to the memory of his father Marco, who inspired him, when a child, the love for these mountains.

References

Albini S., Battaglia D., Bellini G., Bigoni E., Carminati E., Ceriani S., Forcella F., Gosso G., Guizzetti D., Oliva A., Rebay G., Siletto G.B. & Spalla M.I. (1994) - *Alpine deformations and pre-Alpine remnants in the north-eastern Orobic Alps, Southalpine basement.* Proceedings of Symposium "CROP-Alpi Centrali", Quaderni di Geodinamica Alpina e Quaternaria, 25-39, (Montrasio A. & Sciesa E., eds.).

Arthaud F. & Matte P. (1977) - *Late Paleozoic strike-slip faulting in southern Europe and northern Africa: Result of a right-lateral shear zone between the Appalachians and the Urals.* Geological Society of America Bulletin, **88**, 1305-1320.

Bargossi G.M., Berra F., Borsato A., Brack P., Corbari D., Credali M., Ferliga C., Gasparotto G., Marcato E., Marocchi M., Siletto G.B. & Trombetta G.L. (2016) - *Note Illustrative della Carta Geologica d'Italia alla scala 1:50.000 F. 79 Bagolino*. ISPRA, 272 pp.

Bernoulli D. (1964) - *Zur Geologie der Monte Generoso (Lombardische Alpen)*. Beitr. Geol. Karte Schweiz., **118**, 135.

Bernoulli D. & Winkler W. (1990) - *Heavy mineral assemblages from Upper Cretaceous South- and Austroalpine flysch sequences (Northern Italy and Southern Switzerland): source terranes and palaeotectonic implications.* Eclogae Geologicae Helvetiae, **83**, 287310.

Berra F. & Carminati E. (2009) - Subsidence history from a backstripping analysis of the Permo-Mesozoic succession of the Central Southern Alps (Northern Italy*). Basin Research*, **22**, 952-975.

Berra F. & Felletti F. (2011) - *Syndepositional tectonics recorded by soft-sediment deformation and liquefaction structures (continental Lower Permian sediments, Southern Alps, Northern Italy): stratigraphic significance.* Sedimentary Geology, **235**, 249-263.

Berra F., Felletti F. & Tessarollo A. (2016) - *Stratigraphic architecture of a transtensional continental basin in low-latitude semiarid conditions: the Permian succession of the central Orobic Basin (Southern Alps, Italy).* Journal of Sedimentary Research, **86**, 1-22, doi: http://dx.doi.org/10.2110/jsr.2016.26

Berra, F., Galli, M. T., Reghellin, F., Torricelli, S., & Fantoni, R. (2009) - *Stratigraphic evolution of the Triassic-Jurassic succession in the Western Southern Alps (Italy): the record of the two-stage rifting on the distal passive margin of Adria*. Basin Research, **21**, 335-353.

Berra F., Tiepolo M., Caironi V. & Siletto G.B. (2015) - *U-Pb zircon geochronology of the volcanic deposits from the Permian basin of the Orobic Alps (Southern Alps, Lombardy): chronostratigraphic and geological implications*. Geological Magazine, **152**, 429-443, doi:10.1017/S0016756814000405.

Bertotti G., Siletto G.B. & Spalla M.I. (1993) - *Deformation and metamorphism associated with crustal rifting: Permian to Liassic evolution of the Lake Lugano-Lake Como area (Southern Alps).* Tectonophysics, **226**, 271-284.

Blom J. C. & Passchier C.W. (1997) - *Structures along the Orobic thrust, Central Orobic Alps, Italy*. Geologische Rundschau, **86**, 627-636.

Boriani A., Bini A. & Berra F. (2016) - *Note Illustrative della Carta Geologica d'Italia alla scala 1:50.000 F. 56 Sondrio*. ISPRA, 241 pp.

Brack P. (1981) - *Structures in the southwestern border of the Adamello intrusion (Alpi bresciane, Italy).* Schweiz. Mineral. Petrograph. Mitt., **61**, 37-50.

Brodie K.H., Rutter E.H. & Rex D. (1989) - *On the age of deep crustal extensional faulting in the Ivrea Zone, northern Italy*. In: M.P. Coward, M.P., Dietrich D. & Park R.G. (Eds.), Alpine Tectonics. Geol. Soc. London Spec. Pub., **45**, 203-210.

Cadel G. (1986) - *Geology and uranium mineralization of the Collio basin (Central Southern Alps).* Uranium, **2**, 215-240.

Cadel G., Cosi M., Pennacchioni G. & Spalla M.I. (1996) - *A new map of the Permo-Carboniferous cover and Variscan metamorphic basement in the Central Orobic Alps, Southern Alps-Italy*. Memorie di Scienze Geologiche, **48**, 1-53.

Carminati E. & Siletto G.B. (2005) - *The Central Southern Alps (N. Italy) paleoseismic zone: a comparison between field observations and predictions of fault mechanics*. Tectonophysics, **401**, 179-197.

Carminati E., Siletto G. B. & Battaglia D. (1997) - *Thrust kinematics and internal deformation in basement involved foreland fold and thrust belt: the Eastern Orobic Alps case (Central Southern Alps, Northern Italy).* Tectonics, **16**, 259-271, doi: 10.1029/96TC03936.

Casati P. & Gnaccolini M. (1967) - *Geologia delle Alpi Orobie occidentali*. Rivista Italiana di Paleontologia e Stratigrafia, **73**, 25-162.

Cassinis G., Dal Piaz G.V., Eusebio A., Gosso G., Martinotti G., Massari F., Milano P.F., Pennacchioni G., Perello M., Pessina C.M., Roman E., Spalla M.I. & Zerbato M. (1986) - *Report on a structural and sedimentological analysis in the Uranium province of the Orobic Alps, Italy*. Uranium, **2**, 241-260.

Cassinis G. & Perotti C. (1994) - Interazione strutturale permiana tra la linea delle Giudicarie e i bacini di Collio, Tiona e Tragiovo (Sudalpino Centrale, N. Italia). Bollettino della Società Geologica Italiana, **112** (3-4), 1021-1036

Cassinis G., Perotti C. & Ronchi A. (2012) - *Permian continental basins in the Southern Alps (Italy) and peri-mediterranean correlations.* International Journal of Earth Sciences, **101**, 129-157.

Collettini C. (2011) - *The mechanical paradox of low-angle normal faults: Current understanding and open questions.* Tectonophysics, **510**, 253-268.

D'Adda P. & Zanchetta S. (2014) - *Geological-structural map of the Orobic and Porcile thrust junction, central Southern Alps (N Italy)*. Journal of Maps, **11**, 24-38. doi: 10.1080/17445647.2014.944944.

Davis G.H. (1986) - *Shear-zone model for the origin of metamorphic core complexes.* Geology, **11**, 342-347. doi: 10.1130/0091-7613.

De Capitani L., Moroni M. & Rodeghiero F. (1999) - *Geological and geochemical characteristics of Permian tourmalinization at Val Trompia (southern Alps, northern Italy) and relationship with the Orobic tourmalinites*. Periodico di Mineralogia, **68**, 185-212.

Delvaux, D. & Sperner B. (2003) - *New aspects of tectonic stress inversion with reference to the Tensor program.* Geol. Soc. London Spec. Publ., **212**, 75-100.

De Sitter L.U. & De Sitter-Koomans C.M. (1949) - *Geology of the Bergamasc Alps, Lombardy, Italy*. Leidsche Geologische Mededelingen, **14**, 1-257.

Diella V., Spalla M.I. & Tunesi A. (1992) - *Contrasting thermomechanical evolutions in the Southalpine metamorphic basement of the Orobic Alps (Central Alps, Italy).* J. Metam. Geol., **10**, 203-219.

Domeier M. & Torsvik T.H. (2014) - *Plate tectonics in the late Paleozoic.* Geosci. Front., **5**, 303-350.

Edel J.B., Schulmann K., Lexa O. & Lardeaux J.M. (2018) - *Late Palaeozoic palaeomagnetic and tectonic constraints for amalgamation of Pangea supercontinent in the European Variscan belt*. Earth-Science Reviews, **177**, 589-612.

Fantoni R., Bersezio R. & Forcella, F. (2004) - *Alpine structure and deformation chronology at the Southern Alps-Po Plain border in Lombardy.* Bollettino della Società Geologica Italiana, **123**, 463-476.

Forcella F. & Jadoul F. (2000) - *Carta Geologica della Provincia di Bergamo a scala 1:50.000*, Provincia di Bergamo.

Froitzheim N., Derks J.F., Walter J.M. & Sciunnach D. (2008) - *Evolution of an Early Permian extensional detachment fault from synintrusive, mylonitic flow to brittle faulting (Grassi Detachment Fault, Orobic Anticline, southern Alps, Italy).* In: *Tectonic Aspects of the Alpine-Dinaride-Carpathian System* (Siegesmund S., Fugenshuh B. & Froitzheim N., eds). Geological Society, London, Special Publications, 298; 69-82 doi:10.1144/SP298.4.

ISPRA, 2012a, Foglio 077 Clusone, Carta Geologica d'Italia alla, scala 1:50.000.

ISPRA, 2012b, Foglio 056 Sondrio, Carta Geologica d'Italia alla, scala 1:50.000.

Handy M.R. & Zingg A. (1991) - *The tectonic and rheological evolution of an attenuated cross section of the continental crust: Ivrea crustal section, southern Alps, northwestern Italy and southern Switzerland.* Geol. Soc. Am. Bull., **103**, 236-253.

Handy M.R., Franz F., Heller B., Janott B. & Zurbriggen R. (1999) - *Multistage accretion and exhumation of the continental crust (Ivrea crustal section, Italy and Switzerland)*. Tectonics, **18**, 1154-1177.

Hawthorne F.C. & Henry D.J. (1999) - *Classification of the minerals of the tourmaline group*. European Journal of Mineralogy, **11**, 201-215.

Hayman N.W., Knott J.R., Cowan D.S., Nemser E. & Sarna-Wojcicki A. (2003) - *Quaternary low-angle slip on detachment faults in Death Valley, California*. Geology **31**, 343-346.

Lister G.S. & Davis G.A. (1989) - *The origin of metamorphic core complexes and detachment faults formed during Tertiary continental extension in the northern Colorado River region, U.S.A.* Journal of Structural Geology, **11**, 65-94.

Malavieille J. (1993) - *Late Orogenic extension in mountain belts: Insights from the basin and range and the Late Paleozoic Variscan Belt*. Tectonics, **12**(5), 1115-1130.

Malavielle J., Guihot P., Lardeaux J.M. & Gardien V. (1990) - *Collapse of thickened crust in the French Massif: Mont Pilat extensional shear zone and St. Etienne Late Carboniferous basin*. Tectonophysics, **177**, 136-149.

McCann T., Pascal C., Timmermann M. J., Krzywiec P., Lopez-Gomez J., Wetzel A.,

Krawczyk C. M., Rieke H. & Lamarche J. (2006) - *Post-Variscan (end Carboniferous-Early Permian) basin evolution in Western and Central Europe*. **In**: Gee D. G. & Stephenson R. A. (eds) 2006. *European Lithosphere Dynamics.* Geological Society, London, Memoirs, **32**, 355-388.

Marchetti L., Tessarollo A., Felletti F. & Ronchi A. (2017) - *Tetrapod footprint paleoecology: Behavior, taphonomy and ichnofauna disentangled. A case study from the lower Permian of the Southern Alps (Italy).* Palaios, **32**, 506-527.

Martin S., Toffolo L., Moroni M., Montorfano C., Secco L., Agnini C., Nimis P. & Tumiati S. (2017) - Siderite deposits in northern Italy: Early Permian to Early Triassic hydrothermalism in the Southern Alps. Lithos, **284-285**, 276-295.

Marotta A.M., Spalla M. I. & Gosso G. (2009) - *Upper and Lower crustal evolution during lithosphere extension: Numerical modelling and natural footprints from the European Alps*. Geol. Soc. London Special Pub., **321,** 33-72, doi: 10.1144/SP321.3.

Ménard G., & Molnar P. (1988) - *Collapse of Hercynian Tibetan Plateau into a Late Palaeozoic European Basin and Range province*. Nature, **334**, 235-237.

Milano P.F., Pennacchioni G. & Spalla M.I. (1988) - *Alpine and pre-Alpine tectonics in the Central Orobic Alps (Southern Alps)*. Eclogae Geologicae Helvetiae, **81**, 273-293.

Montenat C., Barrier P., Ott d'Estevou P. & Hibsch, C. (2007) - *Seismites: An attempt at critical analysis and classification.* Sedimentary Geology, **196**, 5-30.

Muttoni G., Kent D.V., Garzanti E., Brack P., Abrahamsen N. & Gaetani M. (2003) - Early Permian Pangaea 'B' to Late Permian Pangaea 'A'. *Earth Planet Science Letters,* **215**, 379-394.

Muttoni, G., Mattei, M., Balini, M., Zanchi, A., Gaetani, M. and Berra, F. (2009) - *The drift history of Iran from the Ordovician to the Triassic*. In: *South Caspian to Central Iran Basins* (Brunet M.-F., Wilmsen M. & Granath J.W., Eds.). Geological Society, London, Special Publications, **312,** 7-29.

Petti F.M., Bernardi M., Ashley-Ross M.A., Berra F., Tessarollo A. & Avanzini, M. (2014) - *Transition between terrestrial-submerged walking and swimming revealed by Early Permian amphibian trackways and a new proposal for the nomenclature of compound trace fossil*. Palaeogeography, Palaeoclimatology, Palaeoecology, **410**, 278-289.

Real C., Froitzheim N., Carosi R., & Ferrando S. (2018) - *Evidence of large-scale Mesozoic detachments preserved in the basement of the Southern Alps (northern Lago di Como area)*. Italian Journal of Geosciences, doi: https://doi.org/10.3301/IJG.2017.15.

Schaltegger U. & Brack P. (2007) - *Crustal-scale magmatic systems during intracontinental strike-slip tectonics: U, Pb and Hf isotopic constraints from Permian magmatic rocks of the Southern Alps.* International Journal of Earth Sciences, **96**, 1131-1151.

Schanmugam, G. (2017) - *Global case studies of soft-sediment deformation structures (SSDS): Definitions, classifications, advances, origins, and problems.* Journal of Palaeogeography, **6,** 251-320.

Schönborn, G. (1992) - *Alpine tectonics and kinematic models of the central Southern Alps*. Memorie di Scienze Geologiche, **44**, 229-393.

Slack J.F., Passchier C.W. & Zhang J.S. (1996) - *Metasomatic tourmalinite formation along basement-cover décollements, Orobic Alps, Italy*. Schweiz. Mineral. Petrogr. Mitt., **76**, 193-207.

Spalla M.I. & Gosso G. (1999) - *Pre-Alpine tectonometamorphic units in the central Southern Alps: structural and metamorphic memory.* Memorie di Scienze Geologiche, **51**, 221-229.

Wernicke B. (1981) - *Low angle normal faults in the Basin and Range Province: Nappe tectonics in an extending orogen.* Nature, **291**, 645-648.

Zanchetta S., D'Adda P., Zanchi A., Barberini V. & Villa I.M. (2011) - *Cretaceous-Eocene compressions in the central Southern Alps (N Italy) inferred from* $^{40}Ar/^{39}Ar$ *dating of pseudotachylytes along regional thrust faults*. Journal of Geodynamics, **51**, 245-263, doi: 10.1016/j.jog.2010.09.004.

Zanchetta S., Malusà M. & Zanchi A. (2015) - *Precollisional development and Cenozoic evolution of the Southalpine retrobelt (European Alps).* Lithosphere, **7**, 662-681.

Zanchi A. (1991) - *Tectonic and liquefaction structures in the Loreto basin, Baja California (Mexico): syn-depositional deformation along a fossil fault scarp.* Geodinamica Acta, **5**, 187-202.

ZANCHI A., D'ADDA P., ZANCHETTA S. & BERRA F. (2012) - *Syn-thrust deformation across a transverse zone: the Grem-Vedra fault system (central Southern Alps, N Italy)*. Swiss Journal of Geosciences, **105**, 19-38.

ZANONI D. & SPALLA M.I. (2018) - *The Variscan evolution in the basement cobbles of the Permian Ponteranica Formation by microstructural and petrologic analysis*. Italian Journal of Geosciences, https://doi.org/10.3301/IJG.2018.12

ZANONI D., SPALLA M.I. & GOSSO G. (2010) - *Vestiges of lost tectonic units in conglomerate pebbles? A test in Permian sequences of the Southalpine Orobic Alps*. Geological Magazine **147** (1), 98-122, doi:10.1017/S0016756809990252.

ZHANG J.S., PASSCHIER C.W. & SLACK J.F. (1994) - *Cryptocrystalline Permian tourmalinites of possible metasomatic origin in the Orobic Alps, Northern Italy*. Economic Geology, **89**, 391-396.

ZIEGLER P.A. (1993) - *Late Palaeozoic - Early Mesozoic Plate Reorganization: Evolution and Demise of the Variscan Fold Belt*. In: VON RAUMER J.F. & NEUBAUER F. eds - *Pre-Mesozoic Geology in the Alps*, Springer-Verlag.

Figure captions

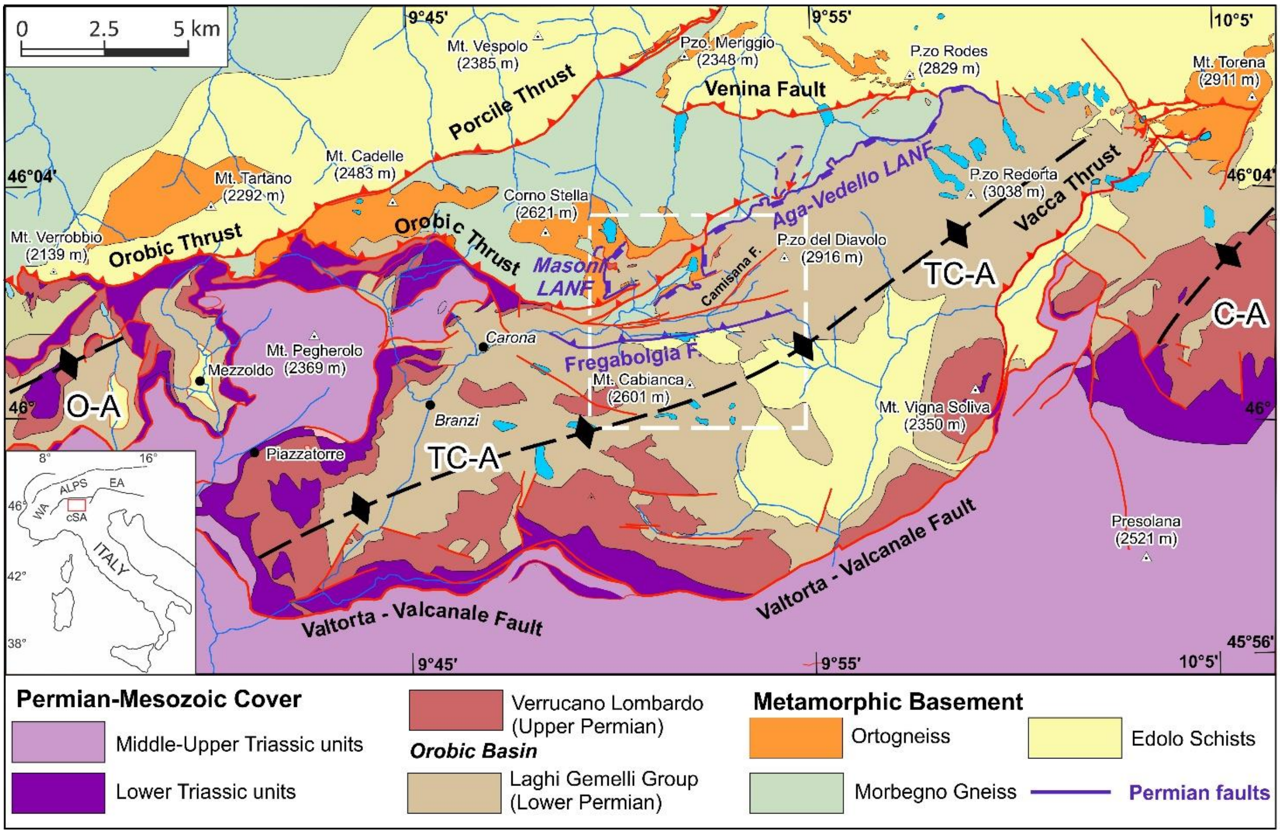

Fig. 1 Structural setting of the northern portion of the central Southern Alps. Data are from our original mapping, from CADEL *et alii*, (1996), ZANCHI *et alii* (2012), FORCELLA & JADOUL (2000), D'ADDA & ZANCHETTA (2014), ZANCHETTA *et alii* (2015). The main Permian faults related with the evolution of the Orobic Basin in blue according to their present-day kinematics (LANF: Low-Angle Normal Fault). The square corresponds to the location of Fig. 2.

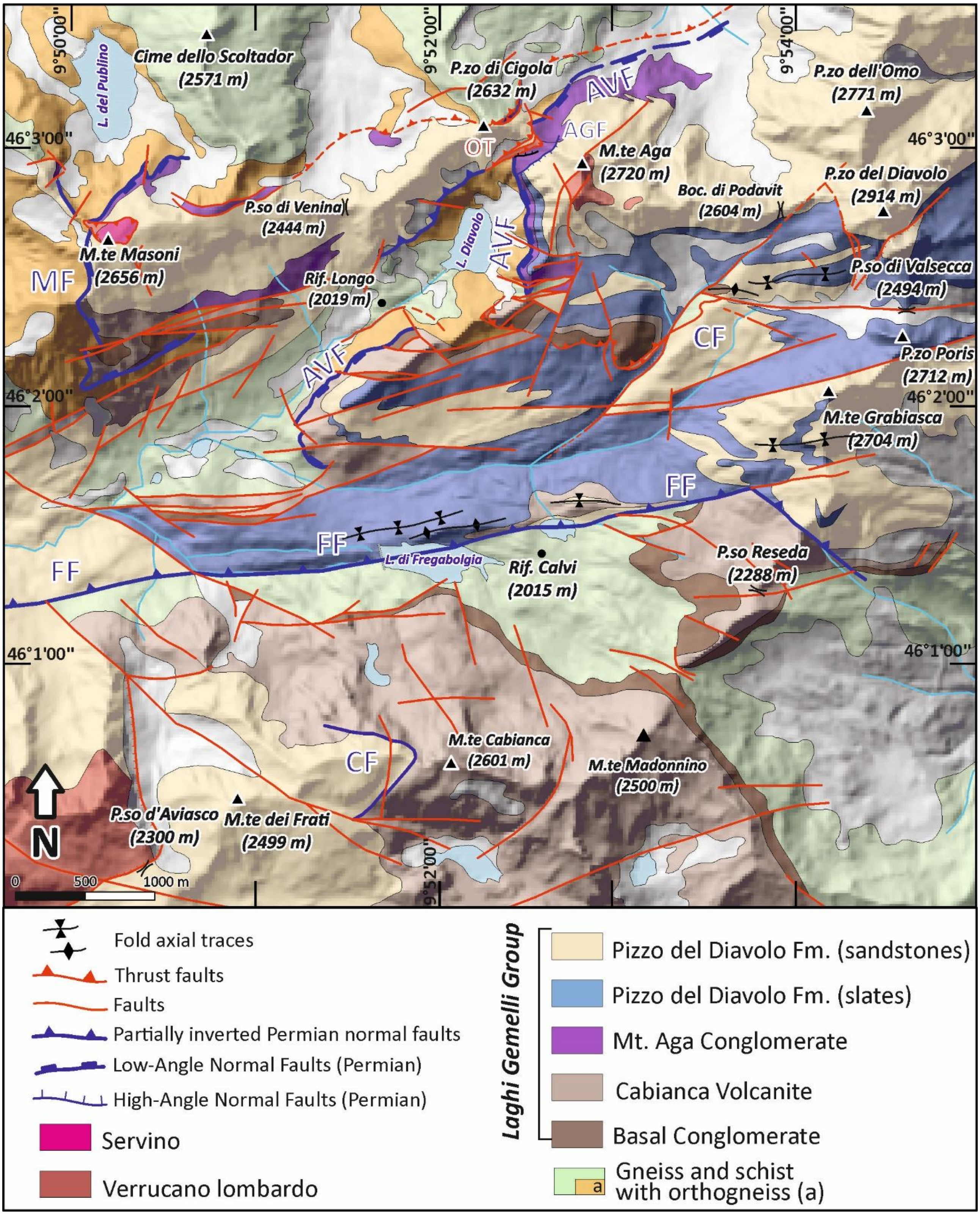

Fig. 2 Geological map of the upper Brembana Valley from CADEL *et alii* (1996) and from our own data. LANF systems occur N and W of Mt. Aga, W and S of Mt. Masoni, and W of Mt. Cabianca. AGF: Aga Growth Fault; AVF: Aga-Vedello Fault; CBF: Cabianca Fault; CF: Val Camisana Fault; FF: Fregabolgia Fault; MF: Masoni Fault.

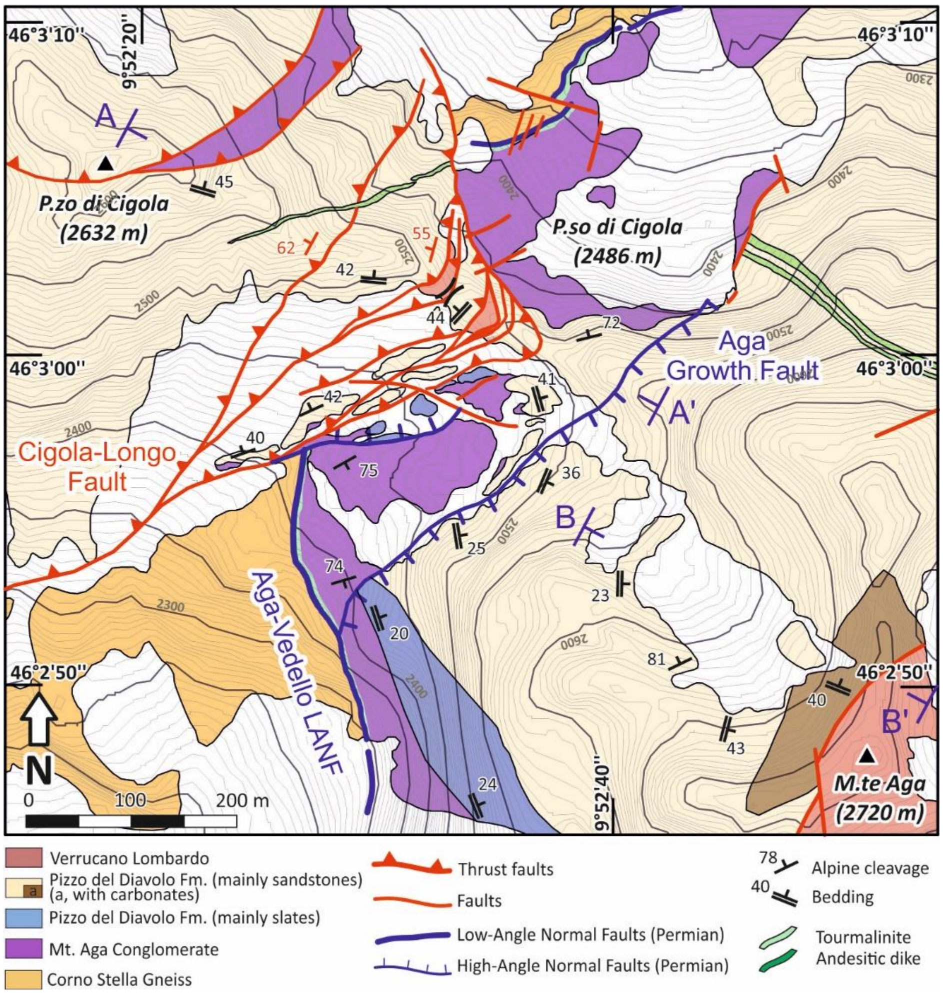

Fig. 3 Detailed geological map of the Aga-Vedello LANF system between the Cigola Pass and Cima Aga. The original survey was performed at a 1: 2,000 scale. Sandstones and slates of the Pizzo del Diavolo Formation overthrust the Aga-Vedello LANF system and its hanging-wall units along the Cigola-Longo Fault.

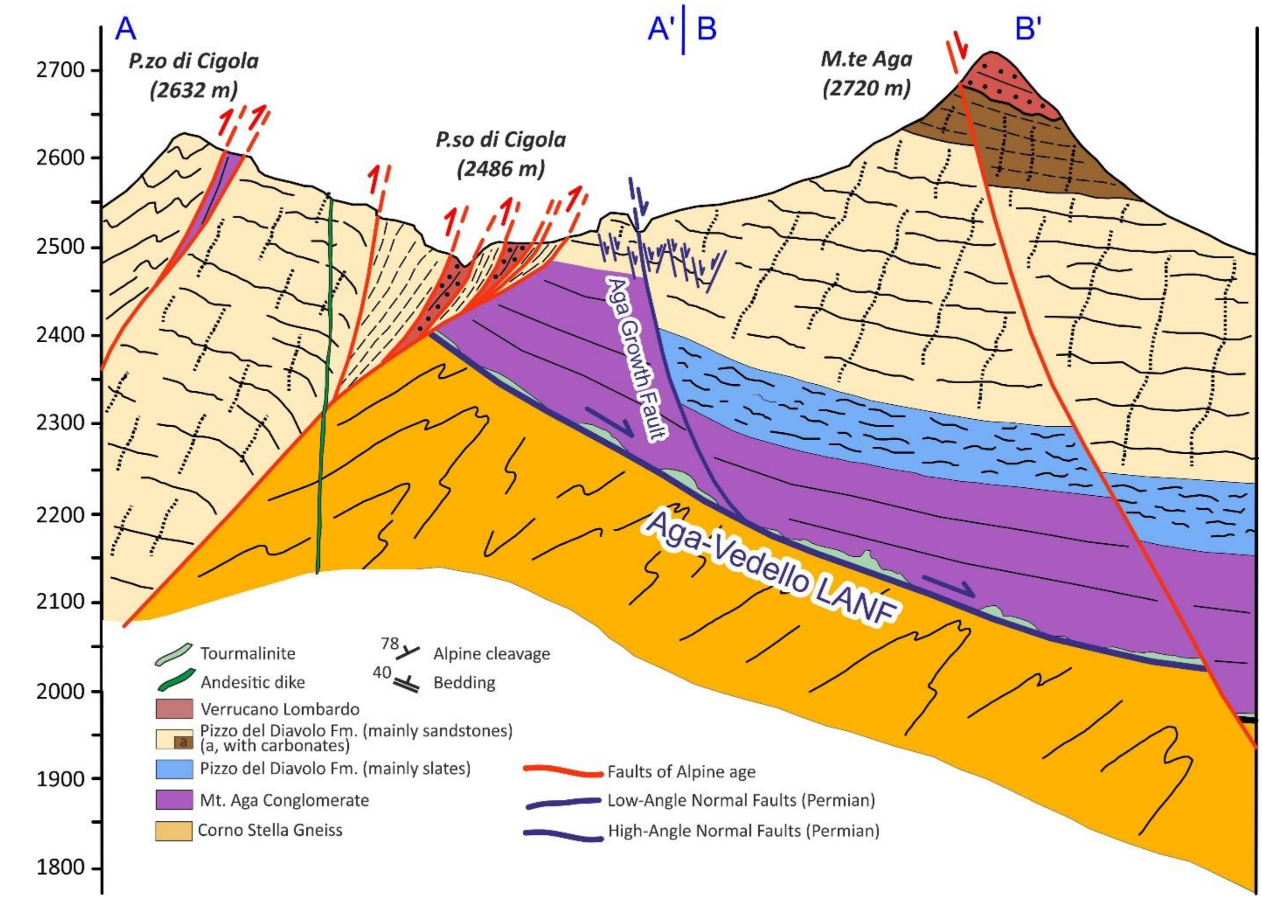

Fig. 4 Cross-section between P.zo Cigola and Mt. Aga (section trace reported in Fig. 3). The Cigola-Longo Fault crosscuts the Aga-Vedello LANF at Cigola Pass. Note that bedding of the Mt. Aga Conglomerate displays a small angle (<15°) with the Aga-Vedello fault surface.

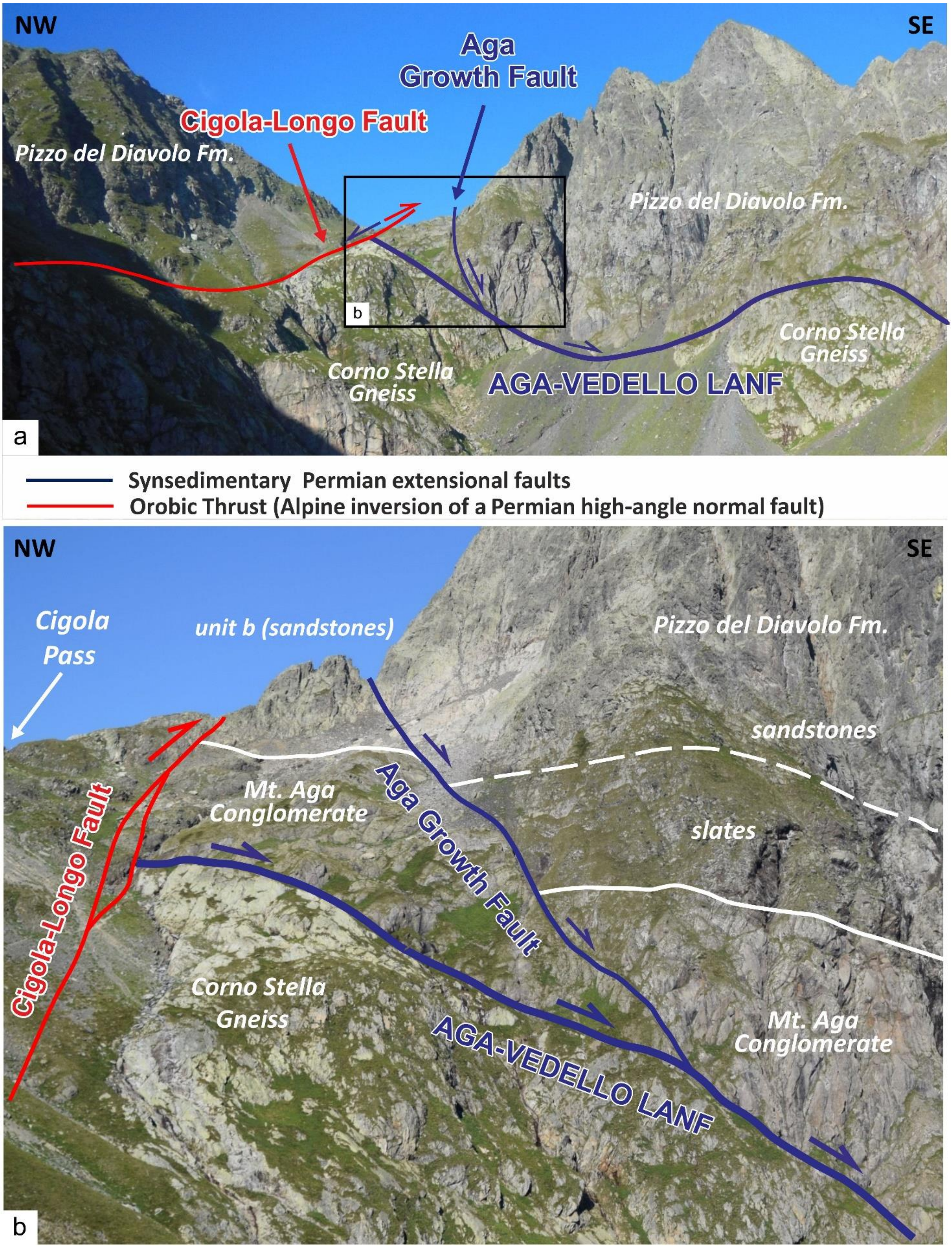

Fig. 5 (a) Panoramic view of the synsedimentary fault system of Mt. Aga, showing its interactions with the Aga-Vedello LANF and with the subsequent Cigola-Longo reverse fault. (b) Detail of Fig. (a).

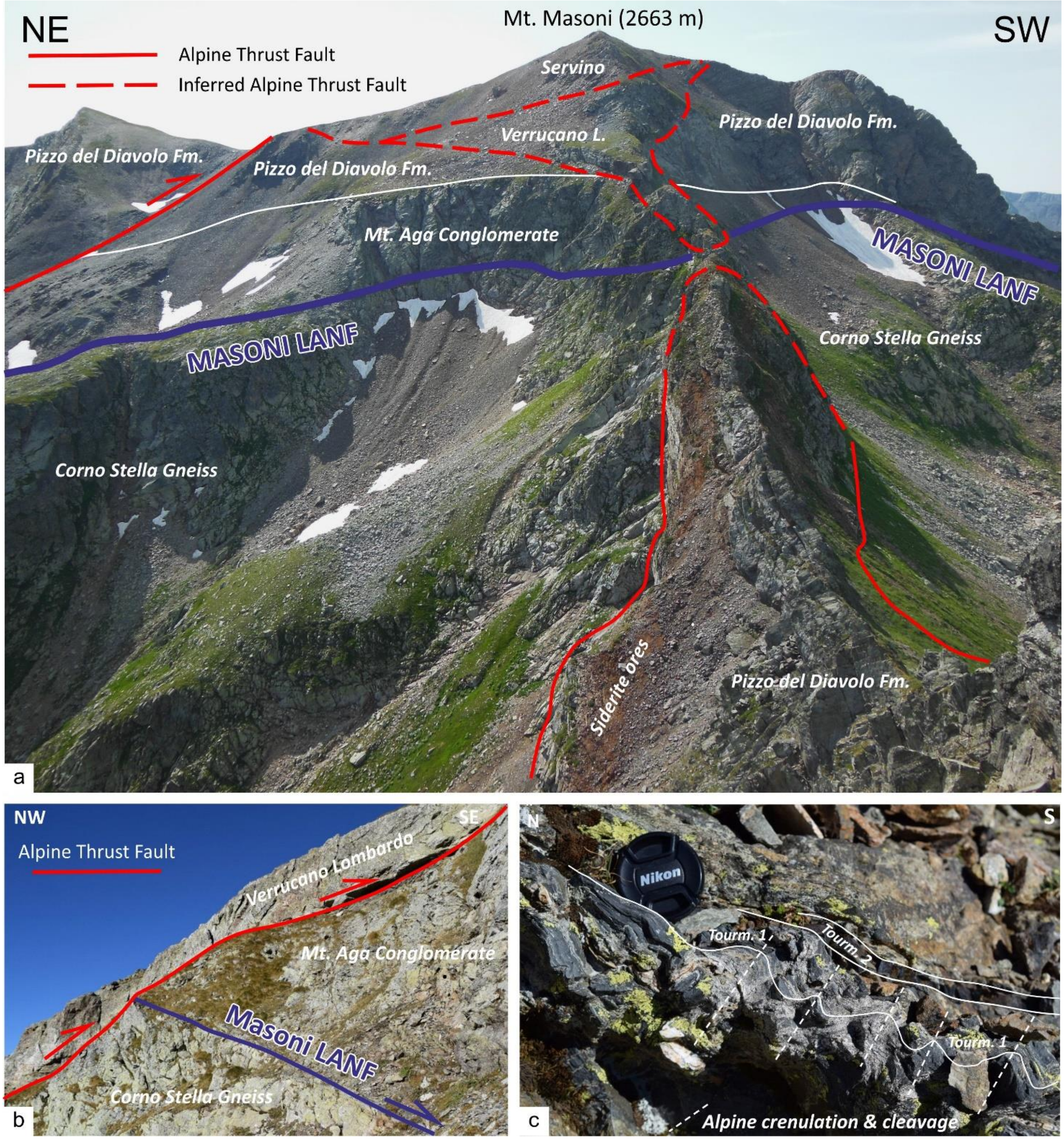

Fig. 6 (a) Panoramic view towards SE of Mt. Masoni with an Alpine thrust sheet that overrides the preserved Masoni LANF. (b) Detail of the Alpine thrust sheet that overrides the Masoni LANF on the SW side of Mt. Masoni. (c) Tourmalinites (Tourm. 1) and cataclasites along the Masoni LANF are frequently affected by the Alpine deformation, resulting in the development of a gentle crenulation sometimes associated to an axial plane cleavage. A second, non-deformed, generation of tourmalinite veins (Tourm. 2) can be tentatively attributed to dissolution and re-precipitation during Alpine tectonics.

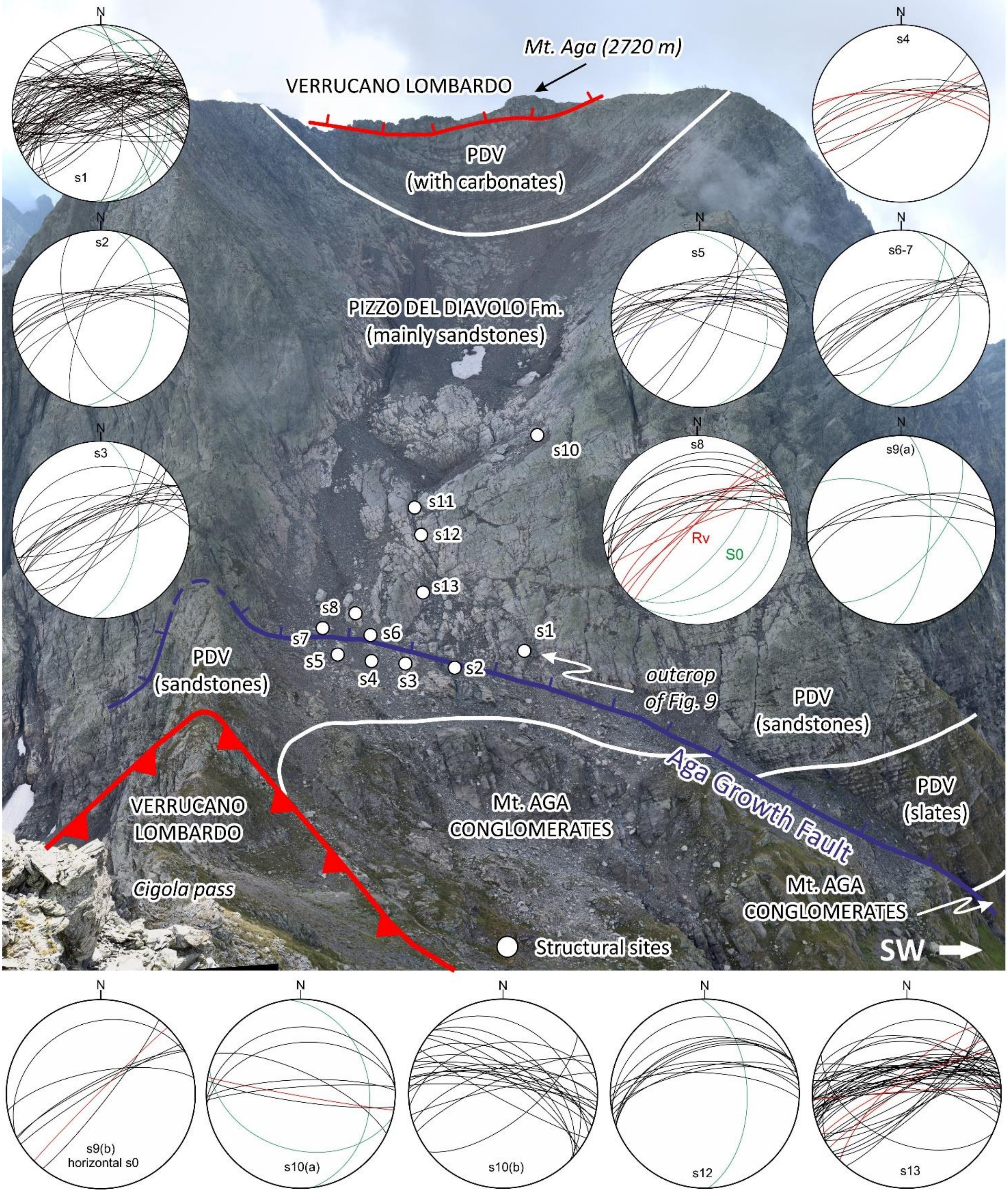

Fig. 7 Location of the studied sites along the western slopes of Mt. Aga, showing the high-angle synsedimentary normal fault recognized in this area (Aga Growth Fault); normal faults in black, reverse faults in blue and bedding planes in red. Tilted conjugate systems can be recognized in several sites. The present-day bedding and faults attitude indicate a tilting, postdating deposition and fault activity resulting in an increase of the average fault dip (65°-80°).

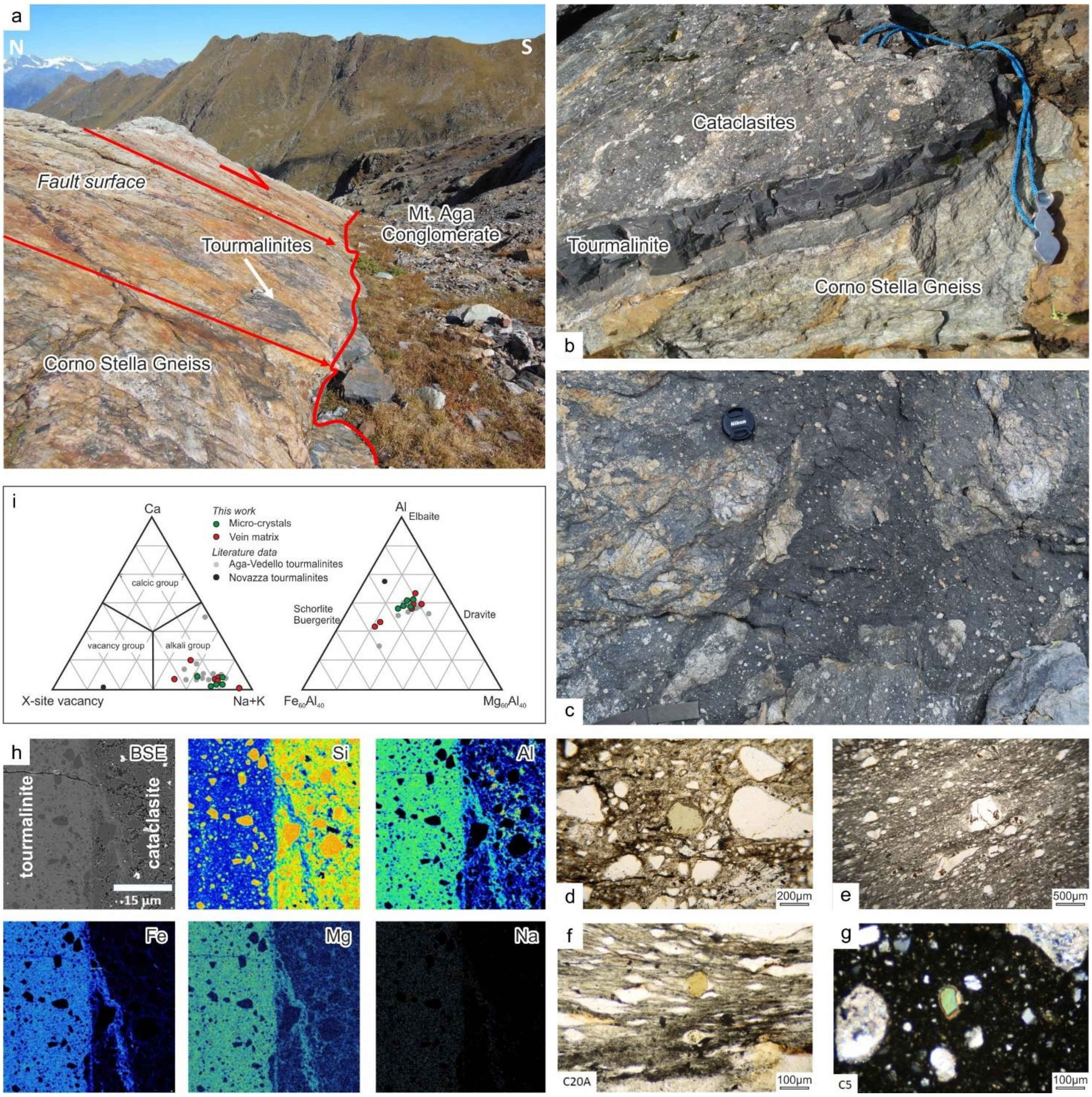

Fig. 8 (a) The exposed fault planes of the Masoni LANF SE of the Publino lake (Fig. 2). (b) Detailed view of the fault zone structure with black aphanitic tourmalinites that impregnated the cataclasites. (c) A view of the fault plane with (sub)rounded clasts of leucocratic gneiss (Corno Stella gneiss) immerged in a grey cataclastic matrix partially metasomatized by tourmalinites (black). (d) Cataclasites, derived from the Corno Stella gneiss containing rounded clast made of polycrystalline quartz, K-feldspar and white mica, in the centre of the image is visible an olive green tourmaline crystal (parallel nicols). (e) Foliated cataclasite (parallel nicols). (f) Along LANF fault segment re-activated during Alpine thrusting a ductile fabric overprints the Permian cataclasites, with fine-grained quartz and sericitic white mica that grow within strain shadows around clasts (parallel nicols). (g) thin rim of newly formed tourmaline grown around a tourmaline clast within the black-coloured tourmalinite matrix (crossed nicols). (h) X-ray element maps across a cataclasite-tourmalinite contact. (i) Chemical composition of tourmalinite matrix and micro-crystals. Literature data are from De Capitani *et alii* (1999).

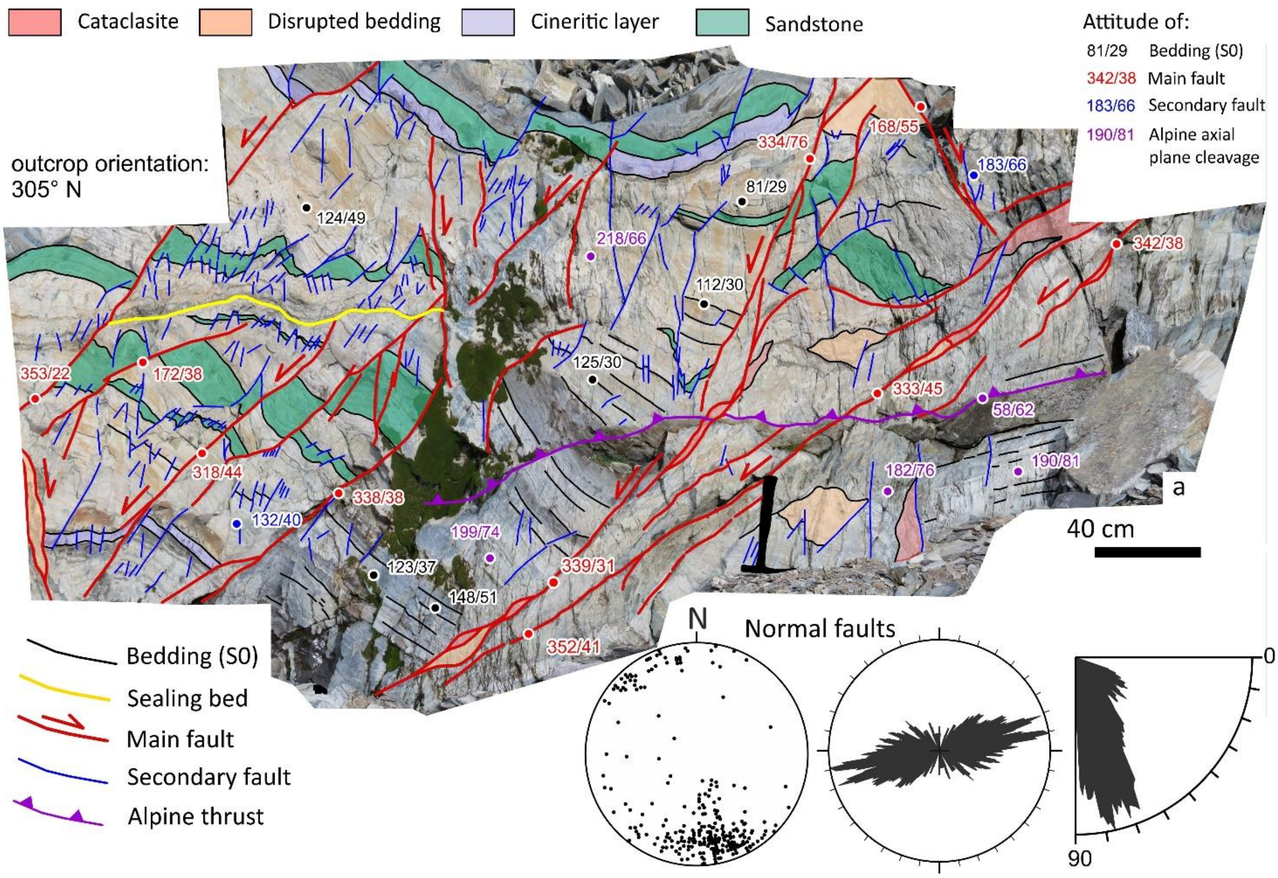

Fig. 9 Structural interpretation of one of the main outcrops (see Fig. 7 for location) along the Aga Growth Fault, in the hanging-wall of the Aga-Vedello LANF, showing the best examples of syntectonic sedimentary structures. Stereoplots represent ca. 250 synsedimentary mesoscopic faults deforming the base of the Pizzo del Diavolo Formation; Schimdt's projection, lower hemisphere. Most of the mesoscopic faults have a normal throw from a few millimetres to a few meters. Rose diagrams refer to the strike and dip of the fault planes. Fault analyses were performed with Win_Tensor (DELVAUX & SPERNER, 2003).

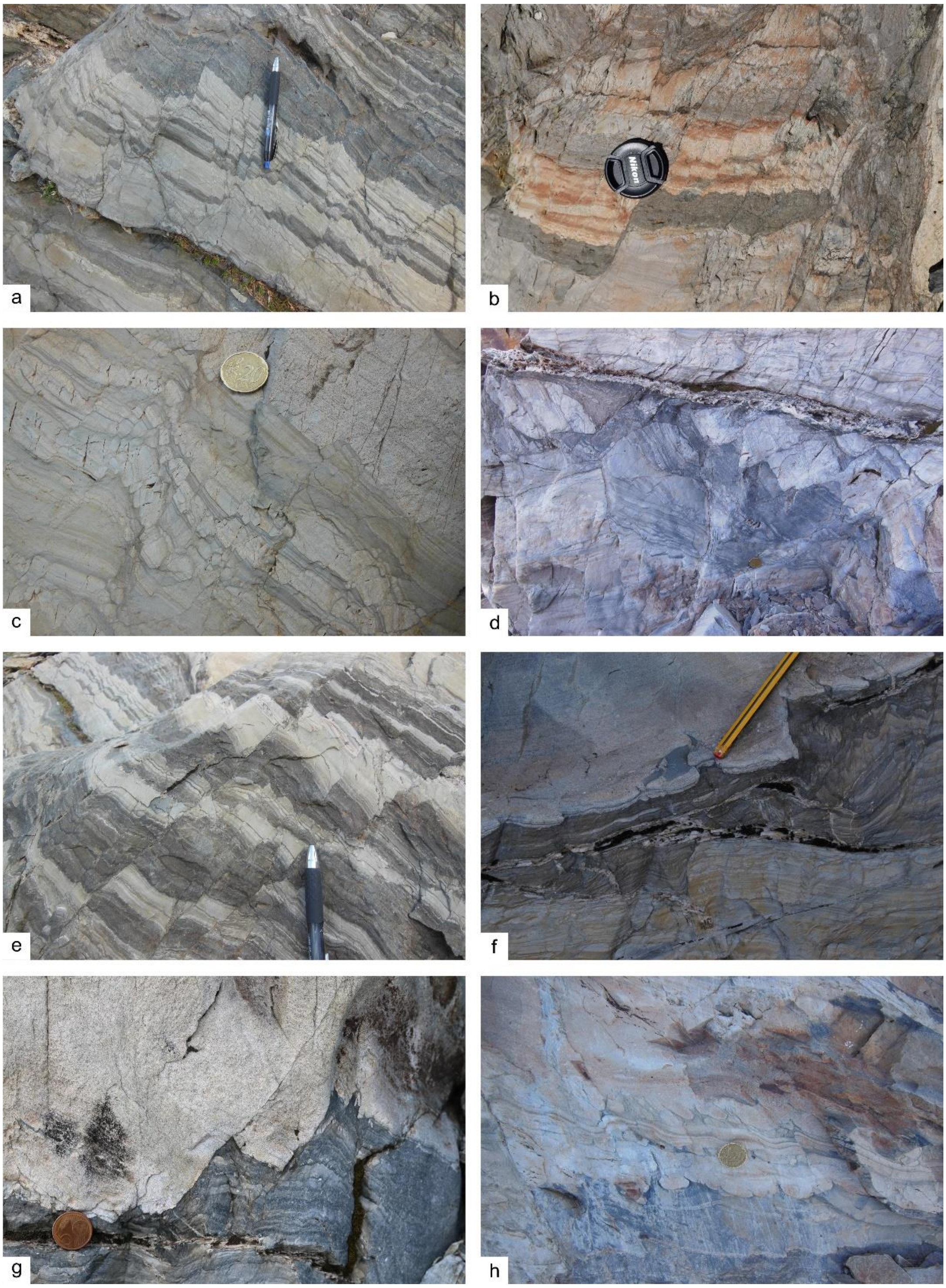

Fig. 10 Detailed field views of the synsedimentary normal faults. (a): planar high-angle normal faults with some of them forming horst-and-graben structures; fault are rotated due to Alpine deformation; (b): high angle normal fault displacing sandstones (yellowish and grey) and siltitic (dark grey, brown) layers; the brown silt layer is partially dragged down along the fault plane; (c) partially disrupted bedding due to normal faults activity; (d) faulted sandstones layers are sealed along a cineritic layer by substantially undisturbed younger layers; (e) a planar high-angle normal fault that caused 1-3 cm of vertical throw; (f) soft-sediment deformation with embryonic ball & pillow structures and injection dikes (centre, lower part of the image); (g) normal faults with flames structures indicating injection of soft-sediments into the coarse layer; (h) displaced balls & pillows structures related to liquefaction phenomena possibly induced by seismic shaking before faulting.

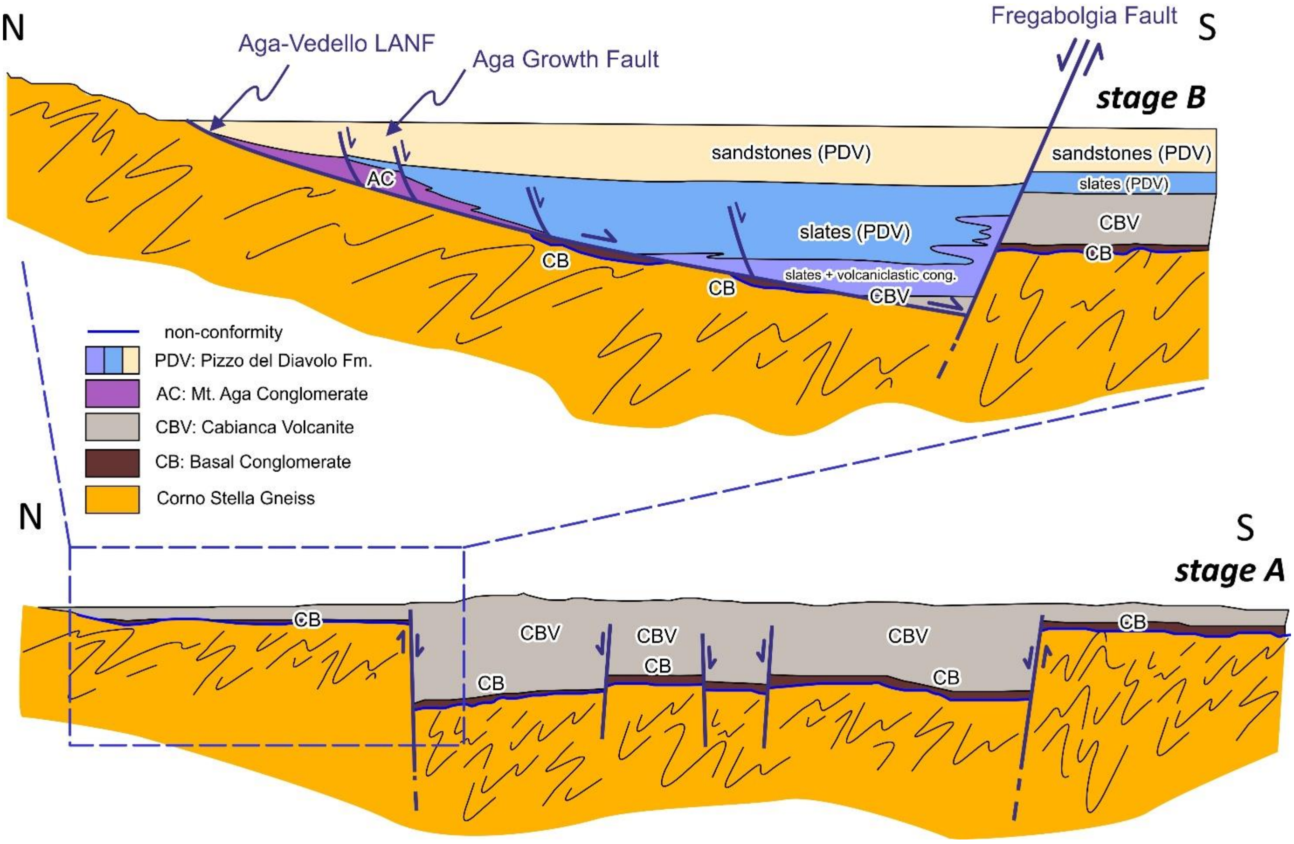

Fig. 11 Schematic cross-section indicating the evolution of the Orobic Basin in the study area between the Aga-Vedello LANF and the Fregabolgia HANF. Stage A shows the formation of a large caldera collapse related to the emplacement of the ignimbrites forming the upper portion of the Cabianca Volcanite, according to CADEL *et alii*. (1996). Stage B illustrates the northward propagation of LANF across the Orobic Basin taking to the formation of an asymmetric half-graben. Field evidence suggests that the throw of the Fregabolgia Fault was already inverted during the E Permian.

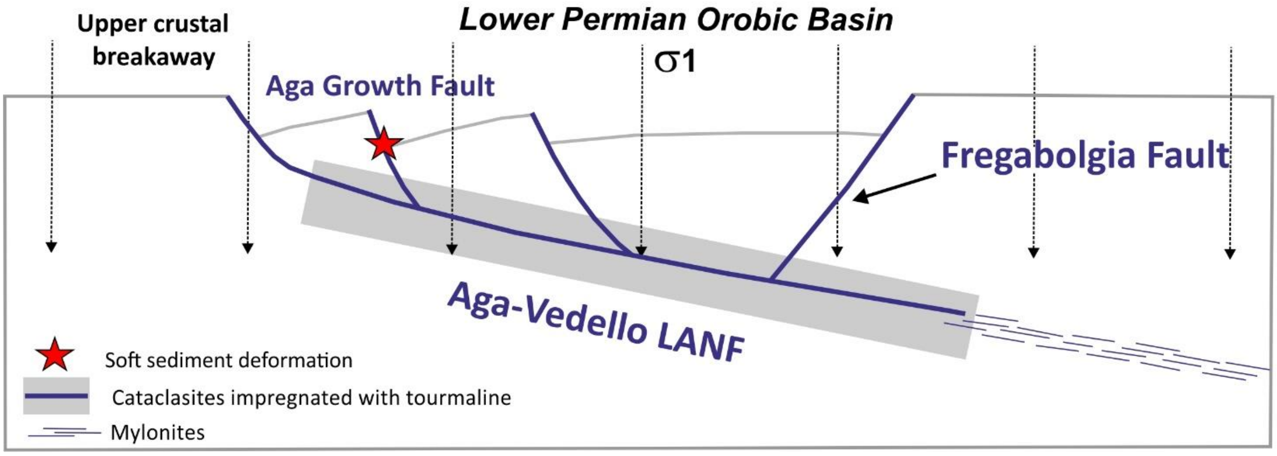

Fig. 12 The Aga-Vedello LANF is interpreted as an upper crustal breakaway (WERNICKE, 1981), with synthetic high-angle normal faults (Aga Growth Fault) soling in the detachment. The structural position of tourmalinites is shown in the section. Modified from COLLETTINI (2011).